Use of Chelating Ligands to Tune the Reactive Site of Half-Sandwich Ruthenium(II)–Arene Anticancer Complexes

Rafael Fernández, Michael Melchart, Abraha Habtemariam, Simon Parsons, and Peter J. Sadler*[a]

Abstract: We show that the chelating ligand XY in Ru^{II} anticancer complexes of the type $[Ru(\eta^6\text{-arene})(XY)Cl]^{n+}$ has a major influence on the rate and extent of aquation, the pK_a of the aqua adduct, and the rate and selectivity of binding to nucleobases. Replacement of neutral ethylenediamine (en) by anionic acetylacetonate (acac) as the chelating ligand increases the rate and extent of hydrolysis, the pK_a of the aqua complex (from 8.25 to 9.41 for arene = *p*-cymene), and changes the nucleobase specificity. For the complexes containing the hydrogen-bond donor en, there is exclusive binding to N7 of guanine in competitive nucleobase reactions, and in the absence of guanine, binding to cytosine or thymine but not to adenine. In contrast, when XY is the hydrogen-bond acceptor acac, the overall affinity for adenosine (N7 and N1 binding) is comparable to that for guanosine, but there is little binding to cytidine or thymidine.

Keywords: antitumor agents · arene ligands · bioinorganic chemistry · nucleobases · ruthenium

Introduction

Organometallic sandwich and half-sandwich complexes offer much potential in drug design.[1] Half-sandwich ruthenium(II)–arene complexes of the type $[Ru(\eta^6\text{-arene})(en)Cl]^+$ (en = ethylenediamine) exhibit anticancer activity both in vitro[2,3] and in vivo,[4] including activity against cisplatin-resistant cancer cells. They bind to DNA oligonucleotides forming monofunctional adducts.[3,5] In aqueous solution, $[Ru(\eta^6\text{-biphenyl})(en)Cl]^+$, for example, binds specifically to guanosine when in competition with adenosine, cytidine, and thymidine monophosphates.[3,6,7] The reaction proceeds through initial aquation of the chloro complex. In the product, guanine is bound to Ru^{II} through N7, with a strong hydrogen bond between C6O and en–NH.[6] Related amino acid[8] and phosphine[9] Ru^{II}–arene complexes are also reported to be cytotoxic. Additional interest in the biological chemistry of Ru complexes[10] arises from clinical trials of the anticancer drugs *trans*-$[RuCl_4(DMSO)(Im)]ImH$ (NAMI-A, in which Im is imidazole)[11] and *trans*-$[RuCl_4(Ind)_2]IndH$ (KP1019, in which Ind is indazole).[12]

Since DNA is a potential target site for Ru^{II}–arene anticancer complexes, it is of interest to investigate features in their design that might allow control of the specificity of binding to nucleobases. The rational design of new DNA binding agents that recognize specific sequences or structures, and can modify specific DNA functions such as replication and transcription, provides an effective approach for the development of novel chemotherapeutic anticancer drugs.[13] We show that incorporation of the anionic *O*,*O*-chelating ligand acetylacetonate (acac) into $\{Ru(\eta^6\text{-arene})\}^{2+}$ complexes leads to significant changes in the recognition of DNA bases relative to the neutral *N*,*N*-chelating ligand en, and also has a major effect on the electronic properties of the Ru^{II}(arene) center and the behavior of the leaving group (Cl^-/H_2O).

Results and Discussion

Complex **1**, $[Ru(\eta^6\text{-}p\text{-cymene})(acac)Cl]$ (Figure 1), was prepared according to a previously published route,[14] and its X-ray crystal structure was determined. The most interesting feature of the structure is the linking of molecules into dimers about an inversion center by pairs of strong acac oxygen···*p*-cymene ring CH hydrogen bonds (O···H3 2.29 Å, cf. van der Waals sum 2.72 Å), as shown in Figure 2 and Table 1. These dimers are linked into a three-dimensional array, principally by Cl1···H6 interactions (2.65 Å, cf. van der Waals sum 2.95 Å).

[a] Dr. R. Fernández, M. Melchart, Dr. A. Habtemariam, Dr. S. Parsons, Prof. Dr. P. J. Sadler
School of Chemistry, University of Edinburgh
West Mains Road, Edinburgh, EH9 3 JJ (UK)
Fax: (+44) 131-650-6453
E-mail: p.j.sadler@ed.ac.uk

 DOI: 10.1002/chem.200400640

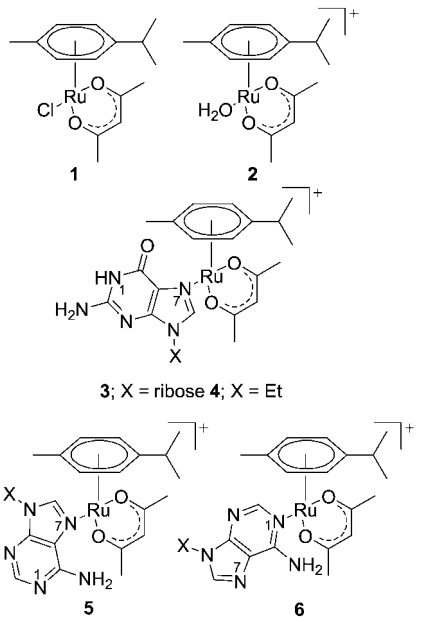

Figure 1. The structures of complexes **1**–**6**. In complexes **3**, **5**, and **6**, X corresponds to a ribose sugar.

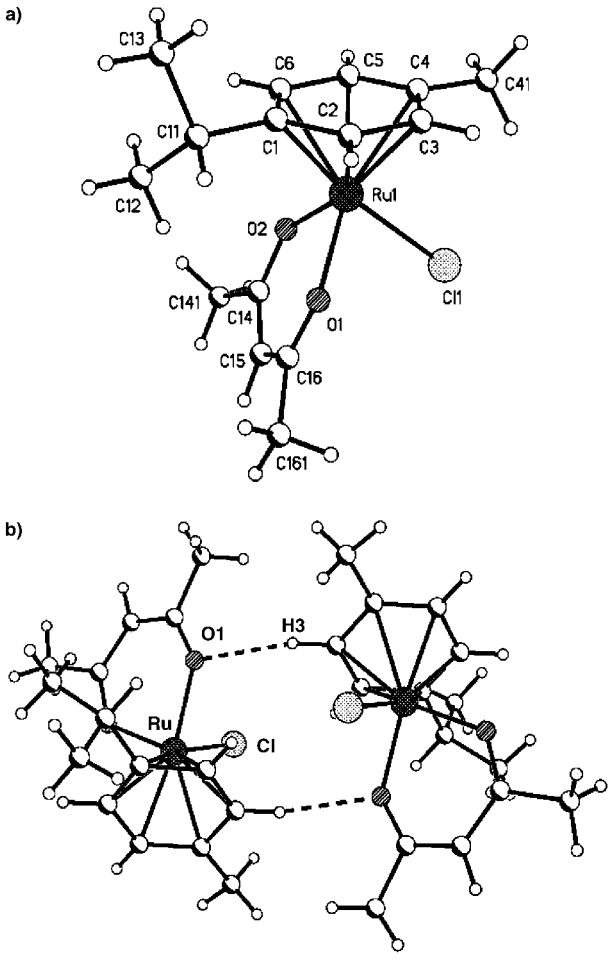

Figure 2. X-ray crystal structure of [Ru(η^6-*p*-cymene)(acac)Cl] (**1**). a) Atom labeling. b) Dimer formed by strong hydrogen bonding between acac oxygen O1 and arene ring H3. The coordinated chloride (Cl1) is involved in hydrogen bonding to H6 of the arene ring of another molecule so linking the dimers into a three-dimensional array.

Table 1. Hydrogen bonding in the X-ray crystal structure of complex **1**. For atom labeling scheme, see Figure 2.

D	H	A	D–H [Å]	H···A [Å]	D···A [Å]	Angle D-H-A [°]
C(2)	H(2)	Cl(1)[a]	0.98	2.79	3.689(2)	153
C(3)	H(3)	O(1)[a]	0.98	2.29	3.234(3)	161
C(6)	H(6)	Cl(1)[b]	0.98	2.65	3.567(2)	155
C(161)	H(161)	Cl(1)[c]	0.98	2.76	3.679(3)	156
C(41)	H(413)	Cl(1)[d]	0.98	2.72	3.380(3)	125

Equivalent positions: [a] $2-x, -y, 2-z$. [b] $3/2-x, 1/2+y, 3/2-z$. [c] $1-x, -y, 2-z$. [d] Intramolecular.

The ^{1}H NMR spectrum of **1** in 10% D_2O/90% H_2O contained a single set of peaks (Figure 3), and conductivity measurements indicated the existence of ionic species in

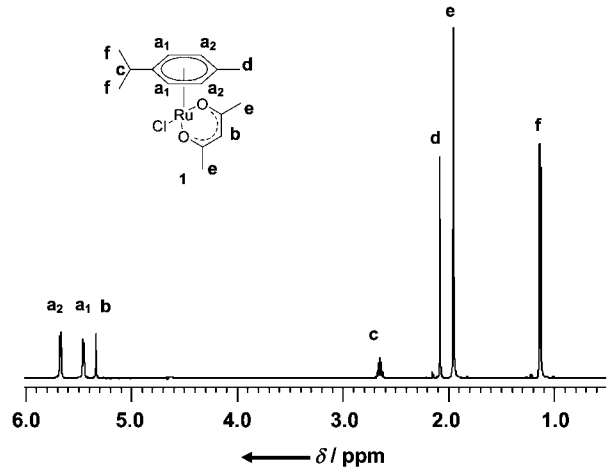

Figure 3. ^{1}H NMR spectrum of complex **1** in 10% D_2O/90% H_2O at 298 K and pH 6.4, with peak assignments indicated.

aqueous solution, suggesting that hydrolysis occurs. This is consistent with the NMR chemical shifts which are very similar to those of the aqua complex **2** (Figure 1), prepared by treatment of **1** with $AgNO_3$. Hydrolysis of **1** appeared to be rapid, since equilibrium was reached by the time the first ^{1}H NMR spectrum was recorded (<5 min). Anation of hydrolyzed **1** was almost complete on addition of NaCl (ca. 1 M; Figure 4). During the titration, the ^{1}H NMR spectra showed only a single set of peaks, indicative of relatively fast exchange on the NMR timescale. Acetylacetonate ligands are known to be strongly electron-donating towards Ru^{II} centers,[15] and the high electron density on Ru^{II} in **2** relative to the analogous en complex makes the substitution of the aqua ligand by negatively charged Cl^- less favorable.[16]

A ^{1}H NMR pH titration of **2** gave a pK_a value of 9.41 for the aqua ligand (Figure 5). This value is considerably higher than that for [Ru(η^6-*p*-cymene)(en)(H_2O)]$^{2+}$, which has a pK_a value of 8.25.[6,7] Thus at physiological pH (7.4), complex **2** would exist mainly as the aqua adduct with little formation of the hydroxo species (which is expected to be less reactive). The pH titration also showed that an additional species was formed above pH 9 (Figure 6), perhaps the dinuclear hydroxo-bridged species [{Ru^{II}(η^6-*p*-cymene)(acac)}$_2$(OH)]$^+$. Hydroxo-bridged {Ru(η^6-arene)}$^{2+}$ com-

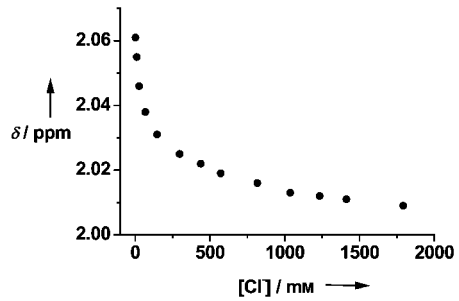

Figure 4. Variation of the ^{1}H NMR chemical shift of the acac Me protons of an hydrolyzed sample of [Ru(η^6-*p*-cymene)(acac)(Cl)] (**1**; 2 mM Ru) on addition of increasing amounts of NaCl. These data, and comparison of shifts with those of the aqua complex **2** prepared by treatment of complex **1** with $AgNO_3$, suggest that **1** hydrolyzes rapidly and almost completely in water.

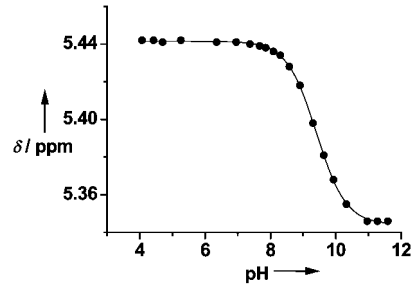

Figure 5. Dependence on pH of the ^{1}H NMR chemical shift of the acac CH resonance of [Ru(η^6-*p*-cymene)(acac)(H_2O)]$^+$ (**2**; 2 mM Ru, 10% D_2O/90% H_2O, 0.1 M $NaClO_4$, 298 K). The line is a computer fit giving pK_a (H_2O) = 9.41 ± 0.01.

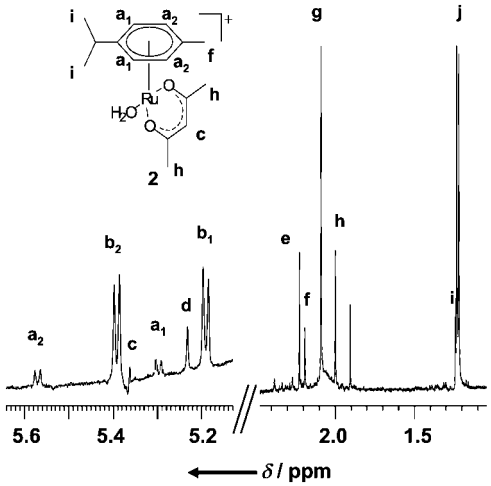

Figure 6. Selected regions of the ^{1}H NMR spectrum of [Ru(η^6-*p*-cymene)(acac)(H_2O)]$^+$ (**2**) in 10% D_2O/90% H_2O at 298 K and pH 10.3, showing the formation of an additional species, possibly [{Ru^{II}(η^6-*p*-cymene)(acac)}$_2$(OH)]$^+$. The region from 5.1 to 5.65 ppm (left) corresponds to the aromatic CH of *p*-cymene. In the region 1.0–2.5 ppm (right), are peaks for the methyl protons of coordinated acac and the methyl groups of *p*-cymene. Peak labels: a_1, a_2 = *p*-cymene CH, **2**; b_1,b_2 = *p*-cymene CH of [{Ru^{II}(η^6-*p*-cymene)(acac)}$_2$(OH)]$^+$; c = acac CH, **2**; d = acac CH of [{Ru^{II}(η^6-*p*-cymene)(acac)}$_2$(OH)]$^+$; e = *p*-cymene Me of [{Ru^{II}(η^6-*p*-cymene)(acac)}$_2$(OH)]$^+$; f = *p*-cymene Me, **2**; g = acac Me_2 of [{Ru^{II}(η^6-*p*-cymene)(acac)}$_2$(OH)]$^+$; h = acac Me_2, **2**; i = *p*-cymene Me_2, **2**; j = *p*-cymene Me_2 of [{Ru^{II}(η^6-*p*-cymene)(acac)}$_2$(OH)]$^+$.

plexes have been reported previously.[17] Below pH 4 some dissociation of the acac ligand was observed (Figure 7). The large increase of 1.2 units in the pK_a value of the aqua ligand in the acac complex **2** relative to the en complex can

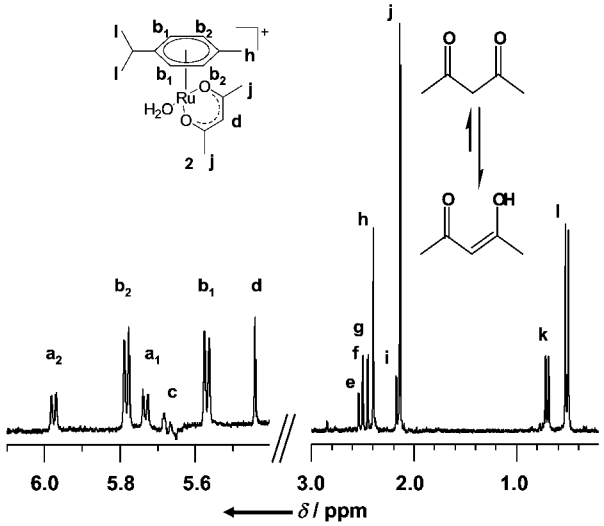

Figure 7. Selected regions of the ^{1}H NMR spectrum of [Ru(η^6-*p*-cymene)(acac)(H_2O)]$^+$ (**2**) in 10% D_2O/90% H_2O at 298 K and pH 2.2, showing the partial dissociation of the acac ligand and possible formation of [Ru(η^6-*p*-cymene)(H_2O)$_3$]$^{2+}$. The region from 5.4 to 6.1 ppm (left) corresponds to the central CH on the acac ligand and the aromatic CH of *p*-cymene. In the region 0.2–3.0 ppm (right) are peaks for the methyl protons of coordinated and free acac, and the methyl groups of *p*-cymene. Peak labels: a_1, a_2 = *p*-cymene CH of [Ru(η^6-*p*-cymene)(H_2O)$_3$]$^{2+}$; b_1,b_2 = *p*-cymene CH, **2**; c = acac CH (free acac); d = acac CH, **2**; e = *p*-cymene Me of [Ru(η^6-*p*-cymene)(H_2O)$_3$]$^{2+}$; f, g = Me (free acac); h = *p*-cymene Me, **2**; i = Me (free acac); j = acac Me_2, **2**; k = *p*-cymene Me_2 of [Ru(η^6-*p*-cymene)(H_2O)$_3$]$^{2+}$; l = *p*-cymene Me_2, **2**.

be rationalized on the basis of the increased electron density on Ru^{II}. Molecular modeling suggested that there could be strong hydrogen bonding between bound water and the oxygen atoms of the acac ligand, as has been suggested to occur in a related complex.[18] This would enhance the stability of the aqua complex **2**.

DNA is a potential target for **1**, which is cytotoxic towards A2780 human ovarian cancer cells,[19] and therefore we investigated the binding of **1** to nucleobases. The binding of complex **1** to guanosine (Guo) was monitored by ^{1}H NMR spectroscopy (1:1 mol ratio, 2 mM, in 90% H_2O/10% D_2O at 298 K and pH 5.3). At equilibrium, approximately 80% of the Guo was bound. Peaks for the Guo adduct (**3**; Figure 1) were observed by the time the first spectrum was recorded (< 5 min after mixing; Figure 8), and there was no change in the ^{1}H NMR spectrum after 24 h, indicating that the equilibrium was reached rapidly. It is well established that N7 of guanine (G) is the preferred nucleotide binding site for many transition metals ions,[20] and metal–N7 binding has been documented by NMR and Raman spectroscopy and by X-ray structural studies on metal–oligonucleotide complexes.[21] Strong and selective binding to G N7 on DNA oligomers has been observed for {Ru(η^6-arene)(en)}$^{2+}$,[3,6] and guanine also binds through N7 to {Ru(η^6-arene)(alanine)}$^+$ and {Ru(η^6-arene)Cl_2} complexes.[8]

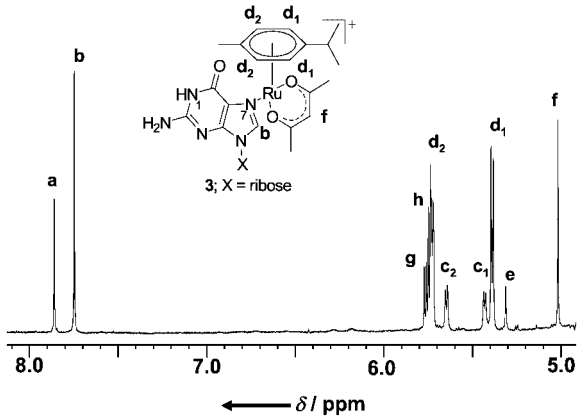

Figure 8. Low-field region of the ^{1}H NMR spectrum of a solution containing guanosine and [Ru(η^6-*p*-cymene)(acac)Cl] (**1**) in a 1:1 mol ratio (2 mM) in 90% H_2O/10% D_2O at 298 K and pH 5.3. The product is [Ru(η^6-*p*-cymene)(acac)(Guo)]$^+$ (**3**). Assignments: a = H8 (free Guo); b = H8, **3**; c = *p*-cymene CH, **2**; d = *p*-cymene CH, **3**; e = acac CH, **2**; f = acac CH, **3**; g = ribose-H1′ (free Guo); h = ribose-H1′, **3**.

A ^{1}H NMR pH titration (Figure 9) was used to confirm that the product is [Ru(η^6-*p*-cymene)(acac)(Guo-*N*7)]$^+$ (**3**). A plot of the H8 chemical shift of **3** versus pH showed an

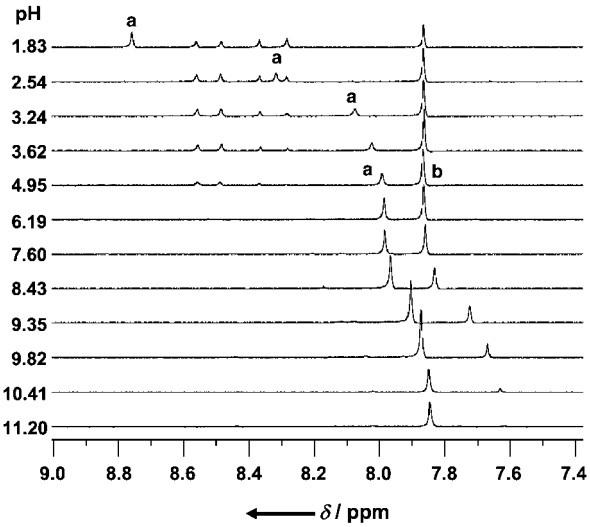

Figure 9. Dependence on pH of the low-field region of the ^{1}H NMR spectrum of **3** in 90% H_2O/10% D_2O, 0.1 M $NaClO_4$, at 298 K. Assignments: a = H8, free Guo; b = H8, **3**.

associated pK_a value of 9.25 (Figure 10), which can be assigned to deprotonation of N1 of coordinated Guo, but no protonation of N7 occurred at acidic pH values (pK_a N7 of Guo is ca. 3). This pK_a value of 9.25 value is almost identical to the literature value for free Guo (9.22)[22] and is therefore unexpectedly high for an N7-coordinated Guo.[7] The peak corresponding to H8 of Guo is shifted upfield by 0.08 ppm with respect to the H8 peak of free Guo, a chemical shift behavior that is atypical for an H8 peak. Metalation at N7 sites of purines by [Ru(η^6-arene)(en)Cl]$^+$ complexes[6,7] and other metal ions usually produces a marked low-field H8 shift of about 0.3–1 ppm.[23] The peak corresponding to the

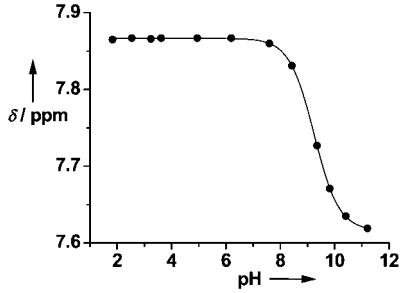

Figure 10. Dependence of the ^{1}H NMR chemical shifts on pH for H8 of [Ru(η^6-*p*-cymene)(acac)(Guo)]$^+$ (**3**; the line is a computer fit giving pK_a (N1H) = 9.25 ± 0.01).

central CH proton on the acac ligand is also shifted upfield, by 0.27 ppm with respect to free **2**. Reactions of 9-ethylguanine (9EtG) with **1** were also studied and gave rise to an analogous adduct **4** (Figure 1). The reaction of complex **1** with 9EtG (1:1 mol ratio) in 10% D_2O/90% H_2O was also followed by ^{1}H NMR spectroscopy (Figure 11). Peaks for

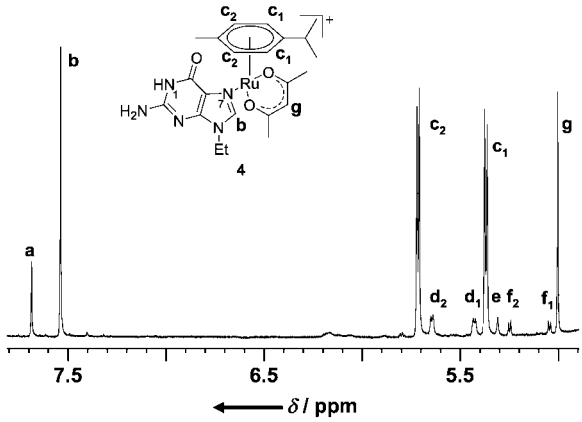

Figure 11. Low-field region of the ^{1}H NMR spectrum of an equilibrium solution containing [Ru(η^6-*p*-cymene)(acac)Cl] (**1**) and 9EtG in a 1:1 mol ratio in 90% H_2O/10% D_2O at 298 K. The product is [Ru(η^6-*p*-cymene)(acac)(9EtG)]$^+$ (**4**). Assignments: a = H8, free 9EtG; b = H8, **4**; c_1,c_2 = *p*-cymene CH, **4**; d_1,d_2 = *p*-cymene CH, **2**; e = acac CH, **2**; f_1,f_2 = *p*-cymene CH of a non-reactive hydroxo form of **2**; g = acac CH, **4**.

the 9EtG adduct (complex **4**; Figure 1) were observed by the time the first spectrum was recorded. There was no further change in the ratio of products and reactants 48 h after mixing. The peak corresponding to the H8 proton of the 9EtG adduct is shifted upfield by 0.15 ppm with respect to the H8 peak of unreacted 9EtG, indicative of 9EtG binding. In addition about 15% free 9EtG and unreacted (hydrolyzed) complex **1** were present in the reaction mixture.

Molecular models suggested that N7 binding of G could be stabilized if N1H-C6O adopted the N1-C6OH tautomeric form allowing hydrogen bonding between an acac O and C6OH (Figure 12). Such a structure may explain the high pK_a value for N1H of coordinated guanosine and contribute to the H8 NMR chemical shift behavior.

The reaction of **1** and adenosine (Ado) in a 1:1 mol ratio in 10% D_2O/90% H_2O at pH 5.8 was monitored by ^{1}H

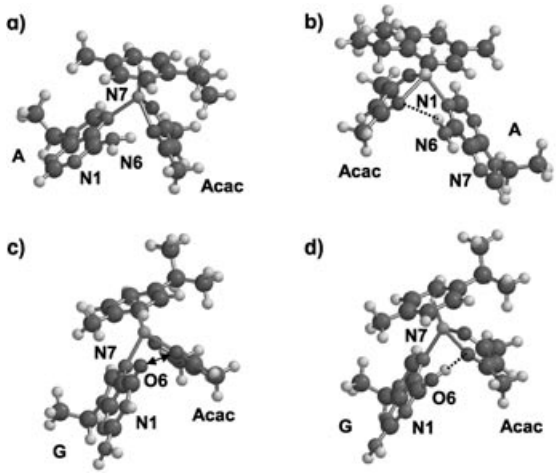

Figure 12. Molecular models of 9-ethylguanine (9EtG) and 9-ethyladenine (9EtA) adducts of $\{Ru(\eta^6\text{-}p\text{-cymene})(acac)\}^+$. a) N7-bound and b) N1-bound 9EtA. c) N7-bound 9EtG as N1H-C6O tautomer and d) N7-bound 9EtG as N1-C6OH tautomer. Hydrogen bonding involving acac oxygen is possible for either N7- or N1-bound 9EtA. In contrast, there is a repulsive interaction between C6O and acac O for N7-bound 9EtG in the N1H–C6O tautomeric form, whereas for the N1-C6OH tautomer, hydrogen bonding is possible.

NMR spectroscopy at 298 K (Figure 13). The resulting spectrum contained three sets of peaks at $\delta = 8.57$ and 8.36 ppm (complex **5**), $\delta = 8.44$ and 8.26 ppm (complex **6**), and $\delta = 8.37$ and $\delta = 8.27$ ppm; the last set corresponding to the H8 and H2 protons of free Ado, respectively, as confirmed by further addition of Ado. The reaction had reached equilibrium by the time the first spectrum was recorded (< 5 min), and the extent of binding was similar to that observed for Guo (ca. 80%). It has been established for adenine derivatives that the intrinsic basicities of N1 and N7 are similar,[22] and that proton binding at N1 decreases metal ion binding

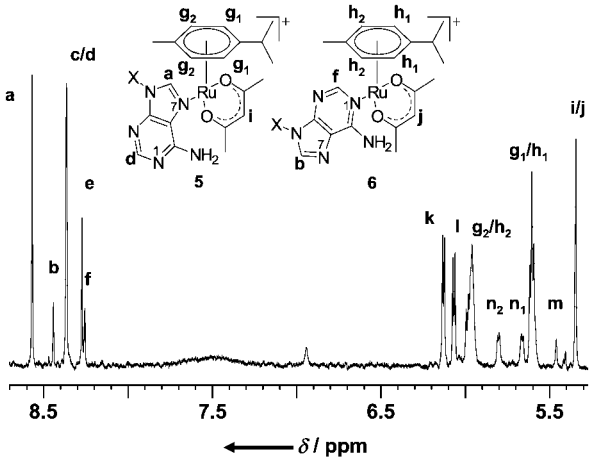

Figure 13. Low-field region of the ^{1}H NMR spectrum of a solution containing $[Ru(\eta^6\text{-}p\text{-cymene})(acac)Cl]$ (**1**) and adenosine in a 1:1 mol ratio in 90% H_2O/10% D_2O at 298 K and pH 5.8. The products are $[Ru(\eta^6\text{-}p\text{-cymene})(acac)(Ado\text{-}N7)]^+$ (**5**) and $[Ru(\eta^6\text{-}p\text{-cymene})(acac)(Ado\text{-}N1)]^+$ (**6**). Assignments: a = H8, **5**; b = H8, **6**; c = H8, free Ado; d = H2, **5**; e = H2, free Ado; f = H2, **6**; g = *p*-cymene CH, **5**; h = *p*-cymene CH, **6**; i = acac CH, **5**; j = acac CH, **6**; k = ribose-H1′, **5** and **6**; l = ribose-H1′, free Ado; m = acac CH, **2**; n = *p*-cymene CH, **2**.

at N7 to the same extent as proton binding at N7 decreases metal ion binding at N1.[24] Plots of the H8 and H2 NMR chemical shifts for bound Ado in complex **5** (Figure 14) showed significant changes between pH 2 and pH 4, from

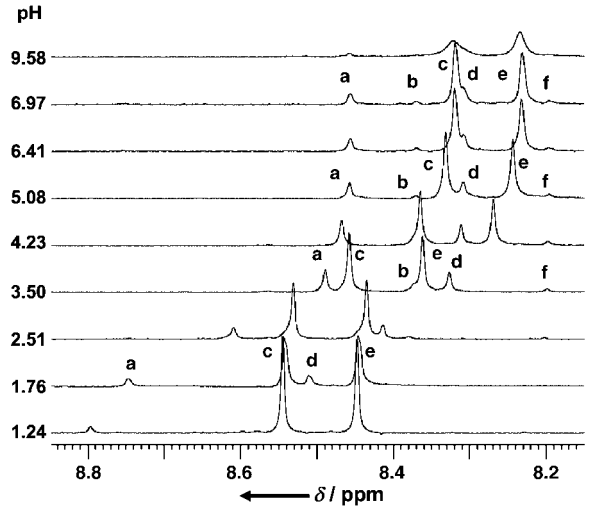

Figure 14. Dependence on pH of the low-field region of the ^{1}H NMR spectrum of a solution containing **5** and **6** in 90% H_2O/10% D_2O, 0.1 M $NaClO_4$ at 298 K. Assignments: a = H8, **5**; b = H8, **6**; c = H8, free Ado; d = H2, **5**; e = H2, free Ado; f = H2, **6**.

which a pK_a value of 2.32 was determined (Figure 15). This corresponds to the protonation of N1 of bound Ado. The pK_a value for N1 of free adenosine was found to be 3.62, in

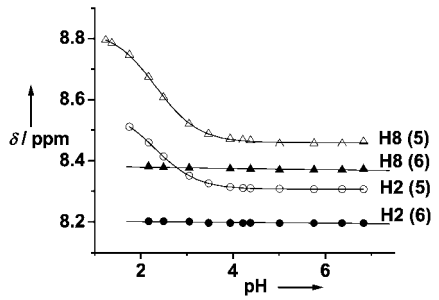

Figure 15. Dependence of the ^{1}H NMR chemical shifts on pH for adenosine complexes **5** and **6** (the lines are computer fits giving pK_a (N1) = 2.32 ± 0.01 for **5**).

agreement with the literature value.[22] From the pH titration, **5** can be assigned as an Ado-N7 adduct, and **6** as an Ado-N1 adduct. The N7/N1 coordination ratio was about 4:1 at pH 5.8. The binding was further confirmed by following the shift of the CH proton of the acac ligand in the ^{1}H NMR spectrum, from $\delta = 5.48$ ppm for unreacted **2** to $\delta = 5.34$ ppm for **5**. Thus changing the chelated ligand L–L in $[Ru(\eta^6\text{-arene})(L\text{–}L)(Cl/H_2O)]^{n+}$ complexes from en to acac has a significant effect on the base selectivity of the $\{Ru(\eta^6\text{-arene})\}^{2+}$ moiety, attributable partly to the difference in hydrogen-bond donor/acceptor properties of the chelating ligands en and acac. Thus, complexes containing

an hydrogen-bond donor, such as en, bind only very weakly to adenine nucleobases.[7] It is evident from molecular models (Figure 12) that $\{Ru(\eta^6\text{-}p\text{-cymene})\}^{2+}$ coordination to adenine can be stabilized by hydrogen bonding between $N6H_2$ as a donor on A and an oxygen atom as hydrogen-bond acceptor on coordinated acac. Unfortunately our attempts to crystallize 9EtG, Guo, and Ado adducts have so far failed.[25]

The competitive binding of **1** to Guo and Ado was also investigated. Equilibrium was reached in less than 5 min when equimolar amounts of Ado and Guo were mixed with **1** in 10% D_2O/90% H_2O, at pH 5.8 (Figure 16). Separate peaks

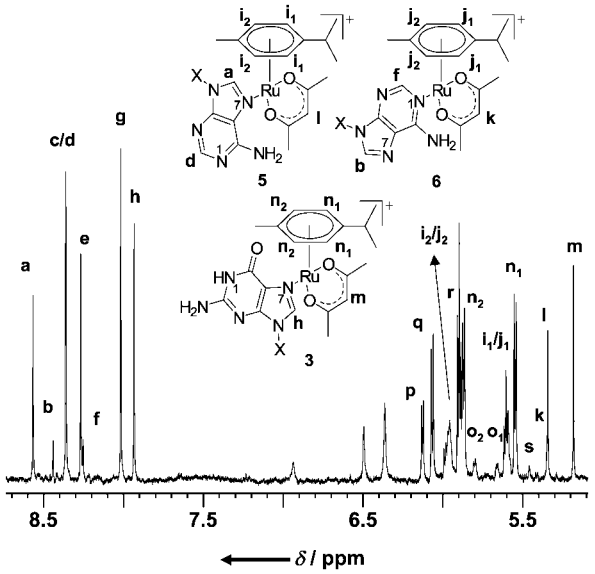

Figure 16. Low-field region of the ^{1}H NMR spectrum of a solution containing adenosine, guanosine and **1** in a 1:1:1 mol ratio in 90% H_2O/10% D_2O at 298 K. The products are $[Ru(\eta^6\text{-}p\text{-cymene})(acac)(Guo\text{-}N7)]^+$ (**3**), $[Ru(\eta^6\text{-}p\text{-cymene})(acac)(Ado\text{-}N7)]^+$ (**5**), and $[Ru(\eta^6\text{-}p\text{-cymene})(acac)(Ado\text{-}N1)]^+$ (**6**). Assignments: a = H8, **5**; b = H8, **6**; c = H8, free Ado; d = H2, **5**; e = H2, free Ado; f = H2, **6**; g = H8, free Guo; h = H8, **3**; i = *p*-cymene CH, **5**; j = *p*-cymene CH, **6**; k = acac CH, **6**; l = acac CH, **5**; m = acac CH, **3**; n = *p*-cymene CH, **3**, o = *p*-cymene CH, **2**; p = ribose-H1′, **5** and **6**; q = ribose-H1′, free Ado; r = ribose-H1′, **3** and free Guo; s = acac CH, **2**.

were observed for free and bound nucleosides, indicative of slow exchange on the NMR timescale and strong binding. The ratio of peaks for Guo-N7/Ado-N7 adducts (**3**:**5**) was approximately 1:1, and since peaks for the Ado-N1 adduct were also present (N7/N1 coordination ratio ca. 4:1), these data suggest that the $\{Ru(p\text{-cymene})(acac)\}^+$ moiety has a slightly higher affinity for Ado compared to Guo under these conditions. However, both Guo and Ado adducts are kinetically labile. Addition of either Ado to a solution of **3**, or Guo to a solution of **5** and **6**, rapidly (< 5 min) resulted in the same equilibrium mixture of adducts as those obtained when complex **1** was reacted directly with Guo or Ado in competition.

^{1}H NMR studies of mixtures of **1** with the pyrimidine nucleosides cytidine and thymidine showed that no adducts were formed over a pH range of 2.4–10.4, in contrast to $[Ru(\eta^6\text{-arene})(en)Cl]^+$ complexes,[7] for which significant binding to N3 was observed. The lack of binding to the acac complex can be ascribed to unfavorable steric and electronic interactions of the nucleobase carbonyl groups with the acac ligand.

Conclusions

In conclusion, we have demonstrated that the chelating ligand in anticancer complexes of the type $[Ru(\eta^6\text{-arene})(chelate)Cl]^{n+}$ has a major influence on the rate and extent of aquation, on the pK_a of the aqua adduct, and on the rate and selectivity of binding to nucleobases. Replacement of neutral en by anionic acac as the chelating ligand increases the rate and extent of hydrolysis, the pK_a of the aqua complex (from 8.25 to 9.41 for arene = *p*-cymene), and changes the nucleobase specificity. For complexes containing the hydrogen-bond donor en, there is exclusive binding to guanine nucleobases in competitive reactions, and in the absence of guanine there is binding to cytosine or thymine, but little binding to adenine bases.[6,7] In contrast when the chelated ligand is the hydrogen-bond acceptor acac, the overall affinity for adenosine can be greater than for guanosine, and there is little binding to cytidine or thymidine. These findings can now be incorporated into design concepts for organometallic Ru^{II}–arene anticancer complexes.

Experimental Section

General: Nucleosides were purchased from Sigma or Aldrich, and D_2O (99.98%) from Aldrich.

^{1}H NMR spectra were acquired on a Bruker DMX 500 (^{1}H = 500 MHz) NMR spectrometer using TBI ^{1}H, ^{13}C, X, or triple resonance H, ^{13}C, ^{15}N probe-heads equipped with *z*-field gradients. All data processing was carried out using XWINNMR version 2.0 (Bruker). ^{1}H NMR chemical shifts were internally referenced to 1,4-dioxane (3.77 ppm) or TSP (0 ppm).

The pH values of the NMR solutions were measured at 298 K directly in the NMR tube, before and after recording NMR spectra, by using a Corning 240 pH meter equipped with an Aldrich micro combination electrode calibrated with Aldrich buffer solutions at pH 4, 7, and 10. The pH values were adjusted with dilute $HClO_4$ and NaOH. No correction was applied for the effect of deuterium on the glass electrode.

^{1}H NMR pH titration curves were fitted using Microcal® Origin®, Version 5.0, from Microcal Software, Inc., with the assumption that the observed chemical shifts are weighted averages according to the population of the protonated and deprotonated species.

Conductivity measurements were carried out on a Hanna Instruments EC 214 Bench Conductivity Meter using 10^{-3} M solutions.

Preparation of $C_{15}H_{21}ClO_2Ru$ (1): Compound **1** was prepared following the method of Carmona et al.[14] $[\{Ru(\eta^6\text{-}p\text{-cymene})Cl_2\}_2]$ (250 mg, 0.41 mmol) and sodium acetylacetonate monohydrate (150 mg, 1.07 mmol) were stirred in acetone (25 mL) at 298 K for 50 min. The solution was then removed in vacuo on a rotary evaporator and the product was extracted with dichloromethane (4 × 5 mL). The solvent was removed again in vacuo by using a rotary evaporator. The final product was recrystallized from acetone/diethyl ether in a freezer at 253 K overnight. The red crystals (180 mg, 0.48 mmol, 59% yield) were collected and dried in vacuo. ^{1}H NMR (500 MHz, $[D_1]CHCl_3$, 298 K, TMS): $\delta = 5.46$ (d, 2H; CH), 5.21 (d, 2H; CH), 5.16 (s, 1H; CH), 2.88 (h, $^3J(H,H) = 7$ Hz, 1H; CH), 2.27 (s, 3H; CH_3), 2.00 (s, 6H; CH_3), 1.33 ppm (d, $^3J(H,H) = 7$ Hz, 6H; CH_3).

Preparation of $C_{15}H_{23}NO_6Ru$ (2): $AgNO_3$ (78 mg, 0.46 mmol) was added to a solution of complex **1** (0.17 g, 0.46 mmol) in H_2O (20 mL). The re-

sulting solution was stirred for 30 min in the dark and then filtered to remove the AgCl formed. Evaporation of the solvent gave the pure product in quantitative yield. ^{1}H NMR (500 MHz, 10% D_2O/90% H_2O, 298 K, TSP): $\delta = 5.78$ (d, 2H; CH), 5.57 (d, 2H; CH), 5.44 (s, 1H; CH), 2.76 (h, $^3J(H,H) = 7$ Hz, 1H; CH), 2.19 (s, 3H; CH_3), 2.06 (s, 6H; CH_3), 1.25 ppm (d, $^3J(H,H) = 7$ Hz, 6H; CH_3).

X-ray crystallography

Complex 1: $C_{15}H_{21}ClO_2Ru$: $M = 369.85$, monoclinic $P2_1/n$, $a = 9.6398(13)$, $b = 13.9993(19)$, $c = 11.5499(16)$ Å, $\beta = 96.619(2)°$, $V = 1548.3(4)$ Å^3, $T = 150$ K, $\rho_{cald} = 1.587$ g cm^{-3}, $\lambda = 0.71073$ Å. Red block of dimensions $0.40 \times 0.31 \times 0.25$ mm^3, $\mu(Mo_{K\alpha}) = 0.242$ mm^{-1}; an absorption correction was performed by the multiscan method using the program SADABS[26] ($0.848 < T < 1$). Data were collected to $2\theta_{max} = 58°$, comprising 9979 measured and 3772 unique data. The structure was solved by direct methods (SIR92[27]) and refined (CRYSTALS[28]) by full matrix least squares against F^2, with anisotropic displacement parameters on all non-H atoms. H-atoms were located in a difference map, but placed in ideal positions and not refined. The final conventional R_1 factor was 0.0289 [based on F and 3429 data with $F > 4\sigma(F)$] and $wR_2 = 0.0720$ (based on F^2 and all data) for 172 parameters. The final difference map max/min were $+0.90/-0.39$ e Å^{-3}, respectively. CCDC 242674 contains the supplementary crystallographic data for this paper. These data can be obtained free of charge via www.ccdc.cam.ac.uk/conts/retrieving.html (or from the Cambridge Crystallographic Data Centre, 12 Union Road, Cambridge CB21EZ, UK; fax: (+44) 1223-336-033; or deposit@ccdc.cam.uk).

Molecular models were constructed using the program Spartan'02 (Wavefunction, Irvine CA, USA) using molecular mechanics (MMFF forcefield) followed by semiempirical molecular orbital (PM3) calculations.

Acknowledgments

We thank the EC (Marie Curie Fellowship for RF), Royal Society, Wolfson Foundation, EPSRC, and Oncosense Ltd for their support for this work; Dr. Duncan Jodrell and colleagues (Cancer Research UK, Western General Hospital, Edinburgh) and EC COST D20 for stimulating discussions; and Ian Hanson and Dr Philip Camp (University of Edinburgh) for assistance with X-ray data collection and molecular modeling, respectively.

[1] R. H. Fish, G. Jaouen, *Organometallics* **2003**, *22*, 2166–2177.
[2] J. Cummings, R. E. Aird, R. Morris, H. Chen, P. del S. Murdoch, P. J. Sadler, J. F. Smyth, D. I. Jodrell, *Clin. Cancer Res.* **2000**, *6* (supplement), abstract 142.
[3] R. E. Morris, R. E. Aird, P. del S. Murdoch, H. Chen, J. Cummings, N. D. Hughes, S. Parsons, A. Parkin, G. Boyd, D. I. Jodrell, P. J. Sadler, *J. Med. Chem.* **2001**, *44*, 3616–3621.
[4] R. E. Aird, J. Cummings, A. A. Ritchie, M. Muir, R. E. Morris, H. Chen, P. J. Sadler, D. I. Jodrell, *Br. J. Cancer* **2002**, *86*, 1652–1657.
[5] O. Novakova, H. Chen, O. Vrana, A. Rodger, P. J. Sadler and V. Brabec, *Biochemistry* **2003**, *42*, 11544–11554.
[6] H. Chen, J. A. Parkinson, S. Parsons, R. A. Coxall, R. O. Gould, P. J. Sadler, *J. Am. Chem. Soc.* **2002**, *124*, 3064–3082.
[7] H. Chen, J. A. Parkinson, R. E. Morris, P. J. Sadler, *J. Am. Chem. Soc.* **2003**, *125*, 173–186.
[8] W. S. Sheldrick, S. Heeb, *Inorg. Chim. Acta* **1990**, *168*, 93–100.
[9] a) C. S. Allardyce, P. J. Dyson, D. J. Ellis, S. L. Heath, *Chem. Commun.* **2001**, 1396–1397; b) C. S. Allardyce, P. J. Dyson, *Platinum Met. Rev.* **2001**, *45*, 62–69.
[10] M. J. Clarke, F. Zhu, D. R. Frasca, *Chem. Rev.* **1999**, *99*, 2511–2533.
[11] a) G. Sava, R. Gagliardi, A. Bergamo, E. Alessio, G. Mestroni, *Anticancer Res.* **1999**, *19*, 969–972; b) G. Sava, E. Alessio, A. Bergamo, G. Mestroni in *Topics in Biological Inorganic Chemistry*, *Vol. 1* (Eds.: M. J. Clarke, P. J. Sadler), Springer, Berlin, **1999**, pp. 143–169.
[12] a) W. Peti, T. Pieper, M. Sommer, B. K. Keppler, G. Giester, *Eur. J. Inorg. Chem.* **1999**, 1551–1555; b) M. Galanski, V. B. Arion, M. A. Jakupec, B. K. Keppler, *Curr. Pharm. Des.* **2003**, *9*, 2078–2089.
[13] a) J. B. Chaires, *Curr. Opin. Struct. Biol.* **1998**, *8*, 314–320; b) T. C. Jenkins, *Curr. Med. Chem.* **2000**, *7*, 99–115.
[14] D. Carmona, J. Ferrer, L. A. Oro, M. C. Apreda, C. Foces-Foces, F. H. Cano, J. Elguero, M. L. Jimeno, *J. Chem. Soc. Dalton Trans.* **1990**, 1463–1476.
[15] T. Hasegawa, T. C. Lau, H. Taube, W. P. Schaefer, *Inorg. Chem.* **1991**, *30*, 2921–2928.
[16] F. Wang, H. Chen, J. A. Parkinson, P. del S. Murdoch, P. J. Sadler, *Inorg. Chem.* **2002**, *41*, 4509–4523.
[17] a) L. A. Oro, M. P. Garcia, D. Carmona, C. Foces-Foces, F. H. Cano, *Inorg. Chim. Acta* **1985**, *96*, L21-L22; b) D. R. Robertson, T. A. Stephenson, *J. Organomet. Chem.* **1976**, *116*, C29–C30; c) T. Arthur, D. R. Robertson, D. A. Tocher, T. A. Stephenson, *J. Organomet. Chem.* **1981**, *208*, 389–400; d) R. O. Gould, C. L. Jones, T. A. Stephenson, D. A. Tocher, *J. Organomet. Chem.* **1984**, *264*, 365–378; e) R. O. Gould, C. L. Jones, D. R. Robertson, D. A. Tocher, T. A. Stephenson, *J. Organomet. Chem.* **1982**, *226*, 199–207; f) W. S. Sheldrick, H.-S. Hagen-Eckard, *J. Organomet. Chem.* **1991**, *410*, 73–84; g) the structure of a monohydroxo-bridged dinuclear palladium complex has also been reported recently: A. Klein, A. Dogan, M. Feth, H. Bertagnolli, *Inorg. Chim. Acta* **2003**, *343*, 189–201.
[18] L. Carter, D. L. Davies, J. Fawcett, D. R. Russell, *Polyhedron* **1993**, *12*, 1599–1602.
[19] R. Aird, M. Melchart, R. Fernández, A. Habtemariam, D. I. Jodrell, P. J. Sadler, unpublished results.
[20] a) R. B. Martin, Y. H. Mariam in *Metal Ions in Biological Systems*, *Vol. 8* (Ed.: H. Sigel), Marcel Dekker, New York, **1979**, pp. 57–124; b) B. Lippert, *Coord. Chem. Rev.* **2000**, *200–202*, 487–516.
[21] J. Sponer, M. Sabat, L. Gorb, J. Leszczynski, B. Lippert, P. Hobza, *J. Phys. Chem. B* **2000**, *104*, 7535–7544, and references therein.
[22] G. Kampf, L. E. Kapinos, R. Griesser, B. Lippert, H. Sigel, *J. Chem. Soc. Perkin Trans. 2* **2002**, 1320–1327.
[23] K. H. Scheller, V. Scheller-Krattiger, R. B. Martin, *J. Am. Chem. Soc.* **1981**, *103*, 6833–6839.
[24] R. Griesser, G. Kampf, L. E. Kapinos, S. Komeda, B. Lippert, J. Reedijk, H. Sigel, *Inorg. Chem.* **2003**, *42*, 32–41.
[25] Note added at proof stage: we have now crystallized complex **5**: the X-ray structure is similar to the model depicted in Figure 12a. The details will be published elsewhere.
[26] G. M. Sheldrick, SADABS, University of Göttingen, Göttingen (Germany), **2004**.
[27] A. Altomare, G. Cascarano, C. Giacovazzo, A. Guagliardi, *J. Appl. Crystallogr.* **1993**, *26*, 343–350.
[28] P. W. Betteridge, J. R. Carruthers, R. I. Cooper, K. Prout, D. J. Watkin, *J. Appl. Crystallogr.* **2003**, *36*, 1487.

Received: June 24, 2004
Published online: September 9, 2004

